



Numerical approximations of singular source terms in differential equations

Anna-Karin Tornberg^{a,*}, Björn Engquist^b

^a *Courant Institute of Mathematical Sciences, New York University, 251 Mercer Street, New York 10012-1185, USA*

^b *Department of Mathematics and PACM, Princeton University, NJ, USA*

Received 13 October 2003; received in revised form 2 April 2004; accepted 15 April 2004

Available online 11 June 2004

Abstract

Singular terms in differential equations pose severe challenges for numerical approximations on regular grids. Regularization of the singularities is a very useful technique for their representation on the grid. We analyze such techniques for the practically preferred case of narrow support of the regularizations, extending our earlier results for wider support. The analysis also generalizes existing theory for one dimensional problems to multi-dimensions. New high order multi-dimensional techniques for differential equations and numerical quadrature are introduced based on the analysis and numerical results are presented. We also show that the common use of distance functions in level-set methods to extend one dimensional regularization to higher dimensions may produce $O(1)$ errors.

© 2004 Published by Elsevier Inc.

1. Introduction

Regularization of singular terms is an important component in many computational techniques, as for example in the vortex method by Chorin [3], the immersed boundary method by Peskin [11], in the front-tracking method by Tryggvason et al. [17] and in connection to the level-set method, see Osher and Fedkiw [9], Sethian [13].

With the exception of the vortex method, these are all techniques for moving interface problems, in which the underlying grid is not adapted to the moving boundaries. The boundaries, or interfaces, are instead represented separately. Singular source terms with support on these interfaces must be discretized on the background grid, which is often uniform. In a finite element setting, the handling of the interface source terms can be done by evaluating the resulting surface integral in the weak formulation [16]. In a finite difference method, an alternative to regularization is to incorporate the jump conditions arising from the singular term into the numerical algorithm, as is done in the immersed interface method by LeVeque

* Corresponding author. Fax: +212-995-4121.

E-mail address: tornberg@cims.nyu.edu (A.-K. Tornberg).

and Li [7]. It is however more commonly done by regularizing the singularity. The discrete vortices in the vortex method are represented by regularized vortex blobs [3,1].

Numerical regularization has been used in a variety of applications. Some of the examples are: simulation of elastic boundaries in blood flow [10,11], immiscible multi-phase flows [9,13,17], dendritic solidification [4,9], subgrid wire modeling in computational electromagnetics [6], discretization in the vortex method [1,3], and segmentation in image processing [9].

The analysis of regularization is less developed, especially in more than one dimension, and the purpose of this paper is to answer some open questions from earlier papers and also to introduce improved methods based on the analysis.

We want to replace the Dirac delta function δ by a more regular function δ_ε , which can be used on standard computational grids in connection to numerical solution of differential equations with singular source terms and quadrature with singular integrands. We are in particular interested in multi-dimensional singular functions.

Let $\Gamma \subset \mathbb{R}^d$ be $d - 1$ dimensional continuous and bounded surface and let S be surface coordinates on Γ . Define $\delta(\Gamma, g, \mathbf{x})$, $\mathbf{x} \in \mathbb{R}^d$ as a delta function of variable strength supported on Γ such that

$$\int_{\mathbb{R}^d} \delta(\Gamma, g, \mathbf{x})f(\mathbf{x}) \, d\mathbf{x} = \int_{\Gamma} g(S)f(\mathbf{X}(S)) \, dS, \tag{1}$$

where $\mathbf{X}(S) \in \Gamma$.

Now assume that the space \mathbb{R}^d is covered by a regular grid

$$\begin{aligned} \{\mathbf{x}_j\}_{j \in Z^d}, \quad \mathbf{x}_j &= (x_{j_1}^{(1)}, \dots, x_{j_d}^{(d)}), \\ x_{j_k}^{(k)} &= x_0^{(k)} + j_k h_k, \quad j_k \in Z, \quad k = 1, \dots, d. \end{aligned} \tag{2}$$

We are interested in Γ with general location relative to the computational grid. Since we will consider fully general Γ there is no restriction if we fix $x_0^{(k)}$ and we will for simplicity let $x_0^{(k)} = 0$, $k = 1, \dots, d$ in the rest of the paper.

One important property with the numerical regularization technique is that this type of regular grids and standard finite difference or finite element methods can be used. Difficulties with the singularities and the geometry of Γ is all taken care of in the design of the regularization.

When regularizing $\delta(\Gamma, g, \mathbf{x})$ by some $\delta_\varepsilon(\Gamma, g, \mathbf{x})$ of compact support, one would like to retain the definition of the delta function in Eq. (1) in a discrete sense up to some order of accuracy. We replace the integral over the domain by a discrete sum and define the discretization error as

$$E = \left| \left(\prod_{k=1}^d h_k \right) \sum_{j \in Z^d} \delta_\varepsilon(\Gamma, g, \mathbf{x}_j)f(\mathbf{x}_j) - \int_{\Gamma} g(S)f(\mathbf{X}(S)) \, dS \right|. \tag{3}$$

With $f \equiv g \equiv 1$, and Γ a curve in \mathbb{R}^2 , the S -coordinate being the arclength along Γ , the error E is the error made in computing the length of the curve. More general g -functions are common for singular source terms where $\delta(\Gamma, g, \mathbf{x})$ represents a physical force along an interface, such as an elastic force or a surface tension force. We shall see that the error term in Eq. (3) also plays an important role in the numerical approximation of differential equations.

Let us first consider a simple one-dimensional regularization, an appropriate scaling of φ_h^I in Fig. 1

$$\delta_\varepsilon(x) = \begin{cases} (x + \varepsilon)/\varepsilon, & -\varepsilon \leq x < 0, \\ (\varepsilon - x)/\varepsilon, & 0 \leq x \leq \varepsilon, \\ 0, & |x| > \varepsilon. \end{cases} \tag{4}$$

The error E can be written as a sum of an analytical error and a quadrature error

$$E = \left| h \sum_{j \in \mathcal{Z}} \delta_\varepsilon(x_j - \bar{x}) f(x_j) - f(\bar{x}) \right| \leq \left| f(\bar{x}) - \int_{\mathbb{R}} \delta_\varepsilon(y - \bar{x}) f(y) dy \right| + \left| \int_{\mathbb{R}} \delta_\varepsilon(y - \bar{x}) f(y) dy - h \sum_{j \in \mathcal{Z}} \delta_\varepsilon(x_j - \bar{x}) f(x_j) \right|.$$

It is possible to check that for regular function $f(x)$ these terms are of order $O(\varepsilon^2)$ and $O((h/\varepsilon)^2)$, respectively [14]. With the scaling $\varepsilon = \sqrt{h}$ the overall approximation is of first order in h . This type of analysis is valid for a wide range of ε values. Raviart [12], performed such an analysis for point sources in multi-dimensions, in connection to particle methods. It can also be extended to multi-dimensions for Dirac delta functions with support on manifolds and to properties connected to differential equations [14,15]. For a very narrow support, the δ_ε function is not sufficiently resolved to analyze the error by splitting it into these two parts. Instead, the error must be analyzed directly, taking into account discrete effects of the computational grid.

For special choices of $\delta_\varepsilon(x)$ and support $(-\varepsilon, \varepsilon)$, the error E is particularly small. If $\delta_\varepsilon(x)$ is given by Eq. (4), with $\varepsilon = h$, E is of the order $O(h^2)$, which can be seen after Taylor expanding $f(x_j)$ around \bar{x} , see Section 2. This and other types of narrow delta approximations with ε proportional to h are computationally convenient and the most common in practice. They are the focus of the analysis in this paper.

Such narrow delta approximations were studied by Beyer and LeVeque [2], in connection the heat equation in one dimension. They introduced discrete moment conditions, and performed a detailed error analysis for a second order finite difference discretization of the equation. Waldén [18] later introduced δ_ε functions obeying higher order moment conditions in one dimension. Such functions had also been introduced earlier, in the context of designing interpolation rules on uniform grids, see Monaghan [8] and the references therein. Compare also to the conditions introduced by Beale and Majda [1] for higher order vortex methods.

A one dimensional δ_ε function satisfies q discrete moment conditions if

$$h \sum_{j=-\infty}^{\infty} \delta_\varepsilon(x_j - \bar{x}) (x_j - \bar{x})^r = \begin{cases} 1, & r = 0, \\ 0, & 1 \leq r < q \end{cases} \tag{5}$$

for all values of \bar{x} . If δ_ε satisfies q moment conditions, we will say that it has a moment order q . Proposition 1 in Section 2.1 states the known result $E \leq Ch^q$ (see also [2]). In this section, we furthermore give examples of regularized δ functions δ_ε and also prove that there exists δ_ε with support of width 2ε with moment order q if and only if $2\varepsilon \geq qh$. In Section 2.2, we extend Proposition 1 to approximations with non-uniform quadrature weights.

There are basically two techniques that are used to extend this type of regularization to the multi-dimensional case for which the singularity is supported on a curve or a surface Γ . One is the product formula following Peskin [11]

$$\delta_\varepsilon(\Gamma, g, x) = \int_{\Gamma} \prod_{k=1}^d \delta_{\varepsilon_k}(x^{(k)} - X^{(k)}(S)) g(S) dS \tag{6}$$

in which δ_{ε_k} corresponds to the one dimensional regularized δ function, and $\mathbf{X}(S) = (X^{(1)}(S), \dots, X^{(d)}(S))$ is a point on Γ .

The other method is based on the distance to Γ , and here

$$\delta_\varepsilon(\Gamma, g, \mathbf{x}) = \tilde{g}(\mathbf{x}) \delta_\varepsilon(d(\Gamma, \mathbf{x})), \tag{7}$$

where $d(\Gamma, \mathbf{x})$ is the closest distance from \mathbf{x} to any point on Γ , and \tilde{g} is an extension from $g(S)$ to a neighborhood of Γ . This technique is commonly used in connection to the level set method since the distance function $d(\Gamma, \mathbf{x})$ is then readily available, see [9,13]. We will in this paper not discuss the method for extending g .

The extension to multi-dimensional delta functions in connection to quadrature is studied in Section 3. For δ_ε defined by the product formula in Eq. (6), we prove that if δ_{ε_k} has a moment order of q , then $E \leq Ch^q$ ($h = \max_k h_k$) independent of dimension, with E as defined in Eq. (3). We give numerical results in two dimensions that include different types of regularizations of singularities supported on curves.

For the regularizations based on the distance function the result is very different. Even if this technique is commonly used it produces $O(1)$ errors in some cases. For certain curves Γ there may be no convergence as $h \rightarrow 0$ if ε is proportional to h . We give both analytical and numerical examples with over 10ε is proportional to h^2 with $0 < \alpha < 1$ there is convergence (see [15]) but $\varepsilon = h$ or $\varepsilon = 2h$ are most common in practice.

Section 3 ends with an extension of the product formula technique to the less singular characteristic functions.

The analysis of quadrature expressions of the form above in Eq. (3) is also useful for the approximation of differential equations

$$L(u) = \delta(\Gamma, g, \mathbf{x}), \quad \mathbf{x} \in \Omega \subset \mathbb{R}^d, \tag{8}$$

where L is a linear differential operator and we assume that u satisfies appropriate initial and boundary conditions.

Let a numerical approximation of (8) have the form

$$L_h(u_h)_j = \delta_\varepsilon(\Gamma, g, \mathbf{x}_j), \quad \mathbf{j} \in \Omega_h, \tag{9}$$

where Ω_h is the index set for the grid points inside Ω . With homogeneous initial and boundary conditions u_h will be a linear combination of the values $\{\delta_\varepsilon(\Gamma, g, \mathbf{x}_j)\}_{j \in \mathbb{Z}^d}$. The linear relation is given by the discrete Greens function G_{jm} and we can write

$$u_h(\mathbf{x}_j) = \left(\prod_{k=1}^d h_k \right) \sum_{\mathbf{m} \in \mathbb{Z}^d} \delta_\varepsilon(\Gamma, g, \mathbf{x}_m) G_{jm}. \tag{10}$$

This is to be compared to the corresponding expression for the analytic solution

$$u(\mathbf{x}) = \int_{\mathbb{R}^d} \delta(\Gamma, g, \mathbf{y}) G(\mathbf{x}, \mathbf{y}) d\mathbf{y}. \tag{11}$$

The difference between $u_h(\mathbf{x}_j)$ in Eq. (10) and $u(\mathbf{x})$ in Eq. (11), is of the form of E in Eq. (3), if we identify G with f . However, the discrete Greens function G_{jm} is typically not simply an evaluation of the Greens function at certain points, but rather in general an approximation to the Greens function to some order of accuracy. Hence, in this case there is an additional source of error, which is determined by the choice of discrete operator L_h in Eq. (9).

In Section 4, we first consider two point boundary value problems for ordinary differential equations

$$-u_{xx} = \delta(x - \bar{x}), \quad 0 \leq x \leq 1$$

with homogeneous boundary conditions. The discrete Greens function for this problem, when discretized by a standard second order finite difference approximation, is the same as the analytic Greens function, i.e., $G_{jm} = G(x_j, x_m)$, where

$$G(x, y) = \begin{cases} x(1 - y), & 0 \leq x \leq y, \\ y(1 - x), & y < x \leq 1 \end{cases}$$

and hence, G_{jm} is linear if $x_j \neq x_m$. We get full accuracy away from $x = \bar{x}$ if δ_ε satisfies two moment conditions ($q = 2$ in Eq. (5)).

We continue by carrying this type of analysis further to various numerical approximations and to partial differential equations. Different numerical approximation of the differential operator may require different δ -function regularizations. We show that full fourth order convergence can be achieved away from the singularity, also in parabolic problems, when a fourth order difference formula of the ordinary differential operator is coupled to a regularization δ_ε with moment order 4 ($q = 4$).

In general, any δ_ε regularization does however produce $O(h)$ errors in a neighborhood of the singularity. Only in special cases, with δ_ε approximations designed to match the chosen difference stencil used to discretize the problem, can this error be reduced to $O(h^2)$. For the standard fourth order approximation, this special function is however only of moment order 2, and the error away from the singularity will in this case only be second order. We study both stationary and time dependent singularity locations ($\delta(x - \bar{x}(t))$) and we give some explanation to some numerical results described in [2,18].

In the end of Section 4, we consider the discretization of an elliptic equation with a source term that has a singular support on a curve Γ in \mathbb{R}^2 . As was discussed above, the regularization δ_ε in one dimension can be extended to the two dimensional case either based on the product formula or on the distance to Γ (Eqs. (6) and (7)). Furthermore, the results obtained regarding the accuracy for the quadrature are also relevant for the accuracy of the discrete solutions to this elliptic equation.

For δ_ε extended by the product rule, the error away from the singularity will be of order p , if we combine a p th order finite difference method with a δ_ε function based on a one dimensional δ_ε function of moment order p . This is confirmed in numerical experiments with $p = 2$ and $p = 4$. Accordingly, the results for the distance formula for the quadrature implies significantly less accurate results.

2. Discrete regularization in one variable

In the following section, we will discuss the discretely regularized multi-dimensional delta functions. These will be based on one-dimensional delta function approximations. We devote this section to give some results for the regularization in one variable, and to introduce some different delta function approximations.

2.1. Discretization error

We begin by introducing the discrete moment conditions.

Definition 2.1. A function $\delta_\varepsilon(x) \in Q^q$ if δ_ε has compact support in $[-\varepsilon, \varepsilon]$, $\varepsilon = mh$, $m > 0$ and

$$M_r(\delta_\varepsilon, \bar{x}, h) = h \sum_{j=-\infty}^{\infty} \delta_\varepsilon(x_j - \bar{x})(x_j - \bar{x})^r = \begin{cases} 1, & r = 0 \\ 0, & 1 \leq r < q \end{cases} \quad (12)$$

for any $\bar{x} \in \mathbb{R}$, where $x_j = jh$, $h > 0$, $j \in \mathbb{Z}$.

The first moment condition, for $r = 0$, ensures that the mass of the delta function is identically 1, independent on shifts in the grid. The higher moment conditions are useful when the delta function is multiplied by a non-constant function, as we will see in the following proposition. This result has also been given in [2].

Proposition 1. Suppose that $\delta_\varepsilon \in Q^q$, $q > 0$ as in Definition 2.1, and $f(x) \in C^q(\mathbb{R})$. Then

$$E = \left| h \sum_{j=-\infty}^{\infty} \delta_\varepsilon(x_j - \bar{x})f(x_j) - f(\bar{x}) \right| \leq Ch^q,$$

and $E = 0$ if f is constant.

Proof. By Taylor expansion follows

$$\begin{aligned} h \sum_{j=-\infty}^{\infty} \delta_\varepsilon(x_j - \bar{x}) f(x_j) &= h \sum_{j=-\infty}^{\infty} \delta_\varepsilon(x_j - \bar{x}) \left[\sum_{p=0}^{q-1} \frac{h^p}{p!} (x_j - \bar{x})^p f^{(p)}(\bar{x}) + O(h^q) \right] \\ &= \sum_{p=0}^{q-1} \frac{h^p}{p!} f^{(p)}(\bar{x}) \left(h \sum_{j=-\infty}^{\infty} \delta_\varepsilon(x_j - \bar{x}) (x_j - \bar{x})^p \right) + O(h^q) \\ &= M_0(\delta_\varepsilon, \bar{x}, h) f(\bar{x}) + \sum_{p=1}^{q-1} \frac{h^p}{p!} f^{(p)}(\bar{x}) M_p(\delta_\varepsilon, \bar{x}, h) + O(h^q). \end{aligned}$$

Since $\delta_\varepsilon \in Q^q$, $q > 0$, $M_0(\delta_\varepsilon, \bar{x}, h) = 1$ and $M_p(\delta_\varepsilon, \bar{x}, h) = 0$, for $p = 1, \dots, q - 1$. From this, the theorem follows.

From this theorem, we see that the number of discrete moment conditions satisfied by the delta function approximation determines the numerical accuracy. The discretization error E can be interpreted as the error made when integrating by the trapezoidal rule, with \bar{x} away from the boundary. It can also be regarded as the error in interpolating f at \bar{x} from the grid values of f , the choice of δ_ε determining the interpolation weights. Hence, δ_ε -functions can be identified with interpolation kernels for interpolation on uniform grids, see [8]. Let us show that it is possible to construct such one dimensional δ_ε functions with any number of correct moments depending on the size of the support.

Theorem 1. *There exists $\delta_\varepsilon \in Q^q$ if and only if $2\varepsilon \geq qh$.*

Proof. Consider first a configuration for which x_{j+1}, \dots, x_{j+n} and only those points are in the support of $\delta_\varepsilon(x - \bar{x})$. Let $y_k = \delta_\varepsilon(x_k - \bar{x})$, $k = j + 1, \dots, j + n$, then $\delta_\varepsilon \in Q^q$ implies

$$A\mathbf{y} = \mathbf{e}_1,$$

where

$$\mathbf{y} = (y_{j+1}, \dots, y_{j+n})^T, \quad \mathbf{e}_1 = (1, 0, \dots, 0)^T$$

and

$$A = \begin{bmatrix} 1 & 1 & \dots & 1 \\ \xi_{j+1} & \xi_{j+2} & \dots & \xi_{j+n} \\ \vdots & \vdots & & \vdots \\ \xi_{j+1}^{q-1} & \xi_{j+2}^{q-1} & \dots & \xi_{j+n}^{q-1} \end{bmatrix}.$$

with $\xi_k = x_k - \bar{x}$, $k = j + 1, \dots, j + n$. The matrix A is of Vandermonde type and of maximal rank. Thus, for any \bar{x} there is a unique solution for $n = q$ and a solution \mathbf{y} depending on $n - q$ parameters for $n > q$.

For $n < q$ consider the matrix A augmented with the column \mathbf{e}_1 . This matrix is also of Vandermonde type for an \bar{x} such that $\xi_k \neq 0$, $k = j + 1, \dots, j + n$ and thus all columns are linearly independent and there is no solution for $A\mathbf{y} = \mathbf{e}_1$.

The theorem now follows since $2\varepsilon \geq qh$ implies that there is at least q points x_k in the support of δ_ε (i.e., $n \geq q$ above). For $2\varepsilon < qh$ there are at most $q - 1$ points x_k in the support ($n < q$).

Remark 2.1. Consider regularizations δ_ε with a fixed number of grid points $n = q$ in its support for some range of \bar{x} . The solution \mathbf{y} and thus δ_ε then depend analytically on the parameters of A and hence on \bar{x} . When the number of grid points in the support n is larger than q , which is typical for some values of \bar{x} , that is no longer true. This results in a piecewise smooth δ_ε . One example is the narrow hat function which will be given below (Eqs. (13) and (14)) which is linear for $-h < x < 0$ and $0 < x < h$ but has a discontinuous derivative at $x = 0$. For some other choices of $2\varepsilon = qh$, there is even less regularity with discontinuities in δ_ε .

As noted above, the most compact δ_ε approximation that obeys q moment conditions may not be continuous. In computations, it is however most practical to deal with continuous δ_ε functions. Define an approximate continuous delta function δ_ε as

$$\delta_\varepsilon(x) = \begin{cases} \frac{1}{h} \varphi_m(x/h), & |x| \leq \varepsilon = mh, \\ 0, & |x| > \varepsilon = mh, \end{cases} \tag{13}$$

where $\delta_\varepsilon \in C(\mathbb{R})$, i.e., $\varphi_m(-m) = \varphi_m(m) = 0$. With this notation, the narrow linear hat function δ_h^L , with $\varepsilon = h$, is defined with

$$\varphi_1^L(\xi) = \min(\xi + 1, 1 - \xi) \tag{14}$$

and the wider hat function δ_{2h}^L ($\varepsilon = 2h$) with

$$\varphi_2^L(\xi) = \frac{1}{4} \min(\xi + 2, 2 - \xi). \tag{15}$$

Furthermore, we define the cosine function δ_{2h}^{cos} ($\varepsilon = 2h$)

$$\varphi_2^{\text{cos}}(\xi) = \frac{1}{4}(1 + \cos(\pi\xi/2)) \tag{16}$$

and a piecewise cubic function, δ_{2h}^C ($\varepsilon = 2h$) with,

$$\varphi_2^C(\xi) = \begin{cases} 1 - \frac{1}{2}|\xi| - |\xi|^2 + \frac{1}{2}|\xi|^3, & 0 \leq |\xi| \leq 1, \\ 1 - \frac{11}{6}|\xi| - |\xi|^2 - \frac{1}{6}|\xi|^3, & 1 < |\xi| \leq 2. \end{cases} \tag{17}$$

This function can also be found in [8,18].

Denote $\bar{x} = x_k + \eta h$, where x_k is the grid point to the left of \bar{x} , and so $\eta \in [0, 1)$. The discrete moments (Definition 2.1) can then be expressed as $M_r(\delta_\varepsilon, \bar{x}, h) = M_r(\varphi_{\varepsilon/h}, \eta)$, where for $m > 0$ integer

$$M(\varphi_m, \eta) = \sum_{j=k-(m-1)}^{k+m} \varphi(j - k - \eta)(j - k - \eta)^r.$$

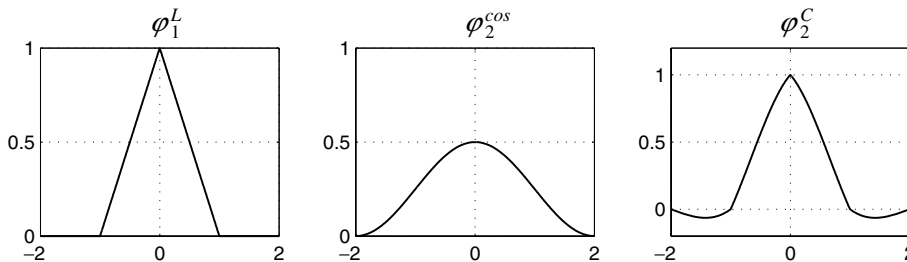


Fig. 1. $\varphi(\xi)$ versus ξ . From left to right, φ_1^L , φ_2^{cos} , φ_2^C , as defined in Eqs. (14), (16) and (17). The integral over each function is 1.

For all the functions given in Eqs. (14)–(17), the mass condition, i.e., the moment condition for $r = 0$ is fulfilled. The first non-zero higher moment for these functions evaluates as follows; for the narrow linear hat function, the wider linear hat function, the cosine function, and the piecewise cubic function, respectively

$$\begin{aligned} M_2(\varphi_1^L, \eta) &= \eta - \eta^2, \\ M_2(\varphi_2^L, \eta) &= \frac{1}{2}(1 + 2\eta - 2\eta^2), \\ M_1(\varphi_2^{\cos}, \eta) &= \frac{1}{2}(1 - \cos(\pi\eta/2) + \sin(\pi\eta/2) - 2\eta), \\ M_4(\varphi_2^C, \eta) &= \eta(1 - \eta)(\eta - 2)(\eta + 1). \end{aligned}$$

From Proposition 1, we have that the error is of $O(h)$ for the cosine function, $O(h^2)$ for the two linear hat functions, and $O(h^4)$ for the piecewise cubic function introduced in (17).

For any choice of φ , such that the delta approximation $\delta_\varepsilon \in \mathcal{Q}^q$, we find that the leading order term of the error can be written $C(\eta)h^q$. Now, consider two grids with resolution h and $h/2$, respectively, and a point \bar{x} such that $\bar{x} = x_k + \eta h$ in the coarse grid. The η value in the fine grid is 2η if $\eta < 1/2$ and $2(\eta - 1/2)$ if $\eta \geq 1/2$, i.e., it is zero for $\eta = 1/2$, which is a grid point in the fine grid. We write $\eta_F = 2(\eta - \frac{1}{2}H(\eta - \frac{1}{2}))$, where H is the Heaviside function. The fraction of the error on the fine grid to the error on the coarse grid is then given by

$$\left| \frac{E(\varphi, f, \eta_F, h/2)}{E(\varphi, f, \eta, h)} \right| = \left| \frac{M_q(\varphi, 2(\eta - \frac{1}{2}H(\eta - \frac{1}{2})))}{M_q(\varphi, \eta)} \right| \frac{1}{2^q} = \frac{\Theta(\eta)}{2^q}. \tag{18}$$

To have convergence order of q that is uniform in h , the quota $\Theta(\eta) = M_q(\varphi, \eta_f)/M_q(\varphi, \eta)$ would need to be a constant, which is not the case. The error is formally $O(h^q)$ ($E \leq Ch^q$), but not uniformly so ($E \neq Ch^q + O(h^q)$), and in numerical tests with comparison of errors on refined grids, this will alter the observed convergence – for some shifts it will be of lower order than q , for other shifts higher.

As noted above, the error for the cosine function δ_{2h}^{\cos} is the largest; it is $O(h)$. In addition, $\Theta_{\cos} \leq |(4 - \pi)/(2 - \pi/\sqrt{2})|$. Therefore, the minimum reduction in error found when doubling the resolution is $2/\max(\Theta_{\cos}) < 1$. Depending on the shift in the grid, the error can even increase after refinement. For the wider hat function δ_{2h}^L , the minimum reduction of the error for one specific refinement is $2^{1.82}$ (formally the error is $O(h^2)$), and for the piecewise cubic function δ_{2h}^C , is 2^3 (formally $O(h^4)$).

This is for a specific shift in the grid. If the error is averaged over many shifts in the grid, the formal order is recovered.

2.2. General quadrature methods

The discretization error E in Proposition 1 can be regarded as the error in the integration of $f(x)\delta(x - \bar{x})$ for some approximation δ_ε , when computed by the trapezoidal rule. The lowest order moment condition in Eq. (12) with $r = 0$ is for example satisfied by $\delta_\varepsilon = \delta_h^L$, the hat function with support $(-h, h)$. With f constant, this condition is sufficient to yield $E = 0$. This moment condition does however not guarantee the correct mass if we compute the integral by Simpson’s rule

$$I_S = h \sum_{j \in \mathbb{Z}} \left(1 + \frac{1}{2}(-1)^j \right) \delta_h^L(x_j - \bar{x}).$$

For example with $\bar{x} = kh$ and k integer, $I_S \neq 1$; for odd k : $I_S = 1.5$ and for even k : $I_S = 0.5$. The remedy is to use a wider support in δ_ε . If δ_h^L is replaced by a hat function with twice the support δ_{2h}^L , then $I_S = 1$ for any

$\bar{x} \in \mathbb{R}$. This can easily be seen directly, but also follows from the following general result for cyclic quadrature methods as, for example the Newton Cotes rules.

Theorem 2. Assume $\delta_\varepsilon \in \mathcal{Q}^q$, $q > 0$ as in Definition 2.1, and $f(x) \in C^q(\mathbb{R})$. Furthermore, assume that the quadrature weights are cyclic with period M such that

$$\sum_{m=1}^M w_m = M,$$

and rescale δ_ε to a function $\delta_{M\varepsilon}$ with support on $[-M\varepsilon, M\varepsilon]$. Then

$$\left| h \sum_{j \in \mathbb{Z}} w_{m(j)} \delta_{M\varepsilon}(x_j - \bar{x}) f(x_j) - f(\bar{x}) \right| \leq Ch^q,$$

where $w_{m(j)}$ is the quadrature weight in grid point j .

Proof. Using that the quadrature rule is cyclic, we can write the sum above as

$$I(f) = h \sum_{j \in \mathbb{Z}} \sum_{m=1}^M w_m \delta_{M\varepsilon}(h(jM + m) - \bar{x}) f(h(jM + m)),$$

using that $X_j = jh$, $h > 0$, $j \in \mathbb{Z}$. Changing the order of the sums, we have

$$I(f) = \sum_{m=1}^M w_m I_m(f), \quad \text{where} \quad I_m(f) = h \sum_{j \in \mathbb{Z}} \delta_{M\varepsilon}(\tilde{x}_j^{(m)} - \bar{x}) f(\tilde{x}_j^{(m)})$$

with $\tilde{x}_j^{(m)} = jH + \tilde{x}_0^{(m)}$, $H = Mh$ and $\tilde{x}_0^{(m)} = mh$.

$\delta_\varepsilon \in \mathcal{Q}^q$ implies $\delta_{M\varepsilon} \in \mathcal{Q}^q$ with step size H , and so Taylor expansion yields (compare the proof of Proposition 1)

$$\begin{aligned} I_m(f) &= \frac{H}{M} \sum_{j \in \mathbb{Z}} \delta_{M\varepsilon}(\tilde{x}_j^{(m)} - \bar{x}) f(\tilde{x}_j^{(m)}) = \frac{1}{M} \left[f(\bar{x}) + \sum_{p=1}^{q-1} \frac{h^p}{p!} f^{(p)}(\bar{x}) M_p(\delta_\varepsilon, \bar{x} - \tilde{x}_0, H) + O(h^q) \right] \\ &= \frac{1}{M} f(\bar{x}) + r_m \end{aligned}$$

with $|r_m| \leq C'h^q$. In total

$$|I(f) - f(\bar{x})| \leq \left| \sum_{m=1}^M \frac{w_m}{M} (f(\bar{x}) + r_m) - f(\bar{x}) \right| \leq MC'h^q \leq Ch^q$$

and the theorem follows.

This observation is important in connection to finite difference discretizations of partial differential equations, when wider difference stencils are used. This will be discussed in Section 4.

3. Multi-dimensional discrete regularization

As was discussed in Section 1, a multi-dimensional regularized delta function can be defined extending a one dimensional delta function approximation δ_ε to several dimensions by either the product rule or by using the distance to Γ (Eqs. (6) and (7)).

In the following two sections, we will discuss these two different approaches. Since they are both based on the one dimensional delta function approximation, the discrete moment conditions and results introduced in Section 2 will be important in the analysis.

3.1. Regularization from product formula

We want to define a delta function approximation in \mathbb{R}^d , and we will do so based on a product of one dimensional delta functions in each coordinate direction. As in Peskin [11], we define

$$\delta_\varepsilon(\Gamma, g, \mathbf{x}) = \int_\Gamma \prod_{k=1}^d \delta_{\varepsilon_k}(x^{(k)} - X^{(k)}(S))g(S) dS \tag{19}$$

with

$$\begin{aligned} \mathbf{x} &= (x^{(1)}, \dots, x^{(d)}) \in \mathbb{R}^d, \\ \mathbf{X}(S) &= (X^{(1)}(S), \dots, X^{(d)}(S)) \in \Gamma, \\ \varepsilon &= (\varepsilon_1, \dots, \varepsilon_d) = (mh_1, \dots, mh_d). \end{aligned}$$

The grid sizes h_1, \dots, h_d refers to the regular grid introduced in Eq. (2).

As a preparation for the forthcoming analysis we introduce a multi-index β , s.t. $|\beta| = \sum_{i=1}^d \beta_i$, and

$$D^\beta f = \frac{\partial^{\beta_1 + \beta_2 + \dots + \beta_d}}{\partial x^{\beta_1} \partial x^{\beta_2} \dots \partial x^{\beta_d}} f. \tag{20}$$

We have the following theorem:

Theorem 3. Suppose that $\delta_\varepsilon \in \mathcal{Q}^q$, $q > 0$, as in Definition 2.1; $g \in C$ and $f \in C^r(\mathbb{R}^d)$, $r \geq q$. Then

$$E = \left| \left(\prod_{k=1}^d h_k \right) \sum_{j \in \mathbb{Z}^d} \delta_\varepsilon(\Gamma, g, \mathbf{x}_j) f(\mathbf{x}_j) - \int_\Gamma g(S) f(\mathbf{X}(S)) dS \right| \leq Ch^q \tag{21}$$

with $h = \max_{1 \leq k \leq d} h_k$ and $E = 0$ for constant f .

Proof. Introducing the definition of $\delta_\varepsilon(\Gamma, g, \mathbf{x}_j)$ in Eq. (19), we have

$$I = \left(\prod_{k=1}^d h_k \right) \sum_{j \in \mathbb{Z}^d} \delta_\varepsilon(\Gamma, g, \mathbf{x}_j) f(\mathbf{x}_j) = \left(\prod_{k=1}^d h_k \right) \sum_{j \in \mathbb{Z}^d} \left[\int_\Gamma \left[\prod_{k=1}^d \delta_{\varepsilon_k}(x_{j_k}^{(k)} - X^{(k)}(S)) \right] g(S) dS \right] f(\mathbf{x}_j).$$

Moving in the summation over j inside the integral, this can be written as

$$I = \int_\Gamma \left[h_1 \sum_{j_1 \in \mathbb{Z}} \delta_{\varepsilon_1}(x_{j_1}^{(1)} - X^{(1)}(S)) \left[h_2 \sum_{j_2 \in \mathbb{Z}} \dots \dots \left[h_d \sum_{j_d \in \mathbb{Z}} \delta_{\varepsilon_d}(x_{j_d}^{(d)} - X^{(d)}(S)) f(\mathbf{x}_j) \right] \dots \right] \right] g(S) dS.$$

From Taylor expansion of $f(\mathbf{x}_j)$ in $x^{(d)}$ around $X^{(d)}(S)$, using $\delta_{\varepsilon_d} \in \mathcal{Q}^q$, similarly to the proof of Proposition 1, the last bracket evaluates as

$$h_d \sum_{j_d \in \mathbb{Z}} \delta_{\varepsilon_d}(x_{j_d}^{(d)} - X^{(d)}(S)) f(\mathbf{x}_j) = f(x_{j_1}^{(1)}, \dots, x_{j_{d-1}}^{(d-1)}, X^d(S)) + \sum_{q \leq p \leq r} \frac{h_d^p}{p!} M_p(\delta_\varepsilon, x^{(d)}, h_d) \frac{\partial^p}{\partial x_d^p} f \Big|_{(x_{j_1}^{(1)}, \dots, x_{j_{d-1}}^{(d-1)}, X^d(S))} + \mathcal{O}(h^{r+1}).$$

Repeating this step for $x^{(d-1)}, \dots, x^{(1)}$ gives

$$I = \int_\Gamma \left[f(\mathbf{X}(S)) + \sum_{q \leq |\beta| \leq r, \beta_i \in R_q} \left[\prod_{i=1}^d \frac{h_i^{\beta_i}}{\beta_i!} M_{\beta_i}(\delta_\varepsilon, X^{(i)}(S), h_i) \right] D^\beta f|_{\mathbf{x}(S)} \right] g(S) \, dS + \mathcal{O}(h^{r+1}).$$

Here we have again used $M_0(\delta_\varepsilon, X^{(i)}(S), h_i) = 1$ and $M_p(\delta_\varepsilon, X^{(i)}(S), h_i) = 0$ for $p = 1, \dots, q - 1, i = 1, \dots, d$, and so $\beta_i \in R_q$ where

$$R_q = \{0, q, q + 1, \dots, r\}.$$

Hence, we have

$$I = \int_\Gamma f(\mathbf{X}(S)) g(S) \, dS + \tilde{E}, \quad |\tilde{E}| \leq Ch^q,$$

where $h = \max_{1 \leq i \leq d} h_i$. Here, we have used that $|\int_\Gamma g(S) \, dS|$ is bounded independent of h . In the special case where f is constant, all derivatives of f are zero, and so $\tilde{E} = 0$. From this, the theorem follows.

Remark 3.1. There is a discrete analogue of Theorem 3. If the integral over Γ is replaced by a discrete sum, both in the definition of δ_ε in Eq. (19) and of E in Eq. (21), the same estimate for E holds. The proof is identical to before, except that the integral over Γ needs to be changed to the discrete sum.

Let us now perform a numerical test. Using the parameter $\theta \in [0, 2\pi]$, the coordinates of the curve $\Gamma \in \mathbb{R}^2$ is defined as

$$(X(\theta), Y(\theta)) = (x_0, y_0) + r(\theta)(\cos(\theta), \sin(\theta)),$$

where

$$r(\theta) = 0.3(1 + 0.2 \sin(2\theta + 5\pi/6) - 0.3 \sin(3\pi + \pi/5)).$$

We numerically very accurately compute the arclength S as a function of θ , and discretize Γ uniformly in S with NC points. Let L denote the length of the curve, and denote the S -values in the discrete points by S_l , such that $S_l = l\Delta S, l = 0, \dots, \text{NC}$ with $\Delta S = L/\text{NC}$, and denote the coordinates of these points by (X_l, Y_l) . Assuming a closed curve, we have $(X_{\text{NC}}, Y_{\text{NC}}) = (X_0, Y_0)$.

Furthermore, we define a computational domain on $(x, y) \in [-0.5, 0.5] \times [-0.5, 0.5]$, with grid size $h = 1/N$ in both directions.

We replace the integral over Γ with a trapezoidal rule, and define

$$\tilde{I}_{g,f}^\Gamma = \Delta S \sum_{l=1}^{\text{NC}} g(S_l) f(X_l, Y_l)$$

with $g(S) \equiv 1$ and $f(x, y) \equiv 1, \tilde{I}_{g,f}^\Gamma$ is the numerical approximation to the length of Γ .

Now we want to measure the error that introducing the approximate delta function creates. Similar to Eq. (19), but replacing the integral over Γ by the trapezoidal rule, we define

$$\delta_\varepsilon(\Gamma, g, \mathbf{x}) = \Delta S \sum_{l=1}^{NC} \delta_\varepsilon(x - X_l) \delta_\varepsilon(y - Y_l) g(S_l). \tag{22}$$

Define the relative error in the numerical computation as

$$E_{\text{rel}} = \left| h^2 \sum_{i,j=0}^N \delta(\Gamma, g, (x_i, y_j)) f(x_i, y_j) - \tilde{I}_{g,f}^\Gamma \right| / |\tilde{I}_{g,f}^\Gamma| \tag{23}$$

with $f(x, y) \equiv 1$, this numerical error is of the size of round off errors. This was expected, according to Theorem 3, and the following remark.

Now, we introduce a non-constant $g(S)$ and $f(x, y) = \tilde{f}(x - x_0, y - y_0)$, where

$$\begin{aligned} g(s) &= 1 + \cos(2\pi s/L + \pi/8) + 3 \sin(4\pi s/L + \pi/3), \\ \tilde{f}(x, y) &= (1 + x + \sin(\pi x))(1 - y + \sin(\pi y))e^{x-y} \end{aligned} \tag{24}$$

with $f(x, y)$ defined this way, the integral over $\delta(\Gamma, g, \mathbf{x})f(x, y)$ is independent of (x_0, y_0) in the definition of Γ . By varying (x_0, y_0) in the numerical computations, we can see the effects the shifts in the grid have on the error.

In Table 1, the relative error is shown for the different delta function approximations introduced in Section 2 in Eqs. (13)–(17). One can note that the two hat functions as well as the piecewise cubic function yield convergence rates very close to the predicted ones. We have $\delta_h^L \in \mathcal{Q}^2$, and $\delta_{2h}^L \in \mathcal{Q}^2$, and can note second order convergence. For the piecewise cubic approximation we have $\delta_{2h}^C \in \mathcal{Q}^4$, and we can note the expected fourth order convergence.

For the cosine approximation, we have $\delta_{2h}^{\text{cos}} \in \mathcal{Q}^1$, and we would expect a first order error. In Table 1 we measure a higher convergence rate in the first refinement, and a lower in the second. To explain this behavior, the error must be studied more carefully (see Fig. 2).

The error expansion for the cosine function can be written as

$$\begin{aligned} E^{\text{cos}} &= h\Delta S \sum_{l=1}^{NC} g(S_l) [f_x(X_l, Y_l)M_1(\varphi_2^{\text{cos}}, \eta_{x,l}) + f_y(X_l, Y_l)M_1(\varphi_2^{\text{cos}}, \eta_{y,l})] \\ &+ \frac{h^2}{2} \Delta S \sum_{l=1}^{NC} g(S_l) [f_{xx}(X_l, Y_l)M_2(\varphi_2^{\text{cos}}, \eta_{x,l}) + f_{yy}(X_l, Y_l)M_2(\varphi_2^{\text{cos}}, \eta_{y,l})] \\ &+ h^2 \Delta S \sum_{l=1}^{NC} g(S_l) [f_{xy}(X_l, Y_l)M_1(\varphi_2^{\text{cos}}, \eta_{x,l})M_1(\varphi_2^{\text{cos}}, \eta_{y,l})] + \mathcal{O}(h^3), \end{aligned}$$

Table 1
The relative error E_{rel} and order of convergence for different δ_ε functions

δ_ε	Relative error (average)			Order of convergence	
	$N = 40$	$N = 80$	$N = 160$	p_{40-80}	p_{80-160}
δ_h^L	1.80×10^{-4}	4.06×10^{-5}	9.53×10^{-6}	2.15	2.09
δ_{2h}^L	6.64×10^{-4}	1.62×10^{-4}	3.99×10^{-5}	2.04	2.02
δ_{2h}^{cos}	4.19×10^{-4}	1.38×10^{-4}	9.74×10^{-5}	1.60	0.50
δ_{2h}^C	6.03×10^{-7}	3.46×10^{-8}	2.09×10^{-9}	4.12	4.05

The error has been computed averaging over 64 shifts in the grid, i.e., small shifts in (x_0, y_0) in the definition of Γ and $f(x, y)$. NC = 100.

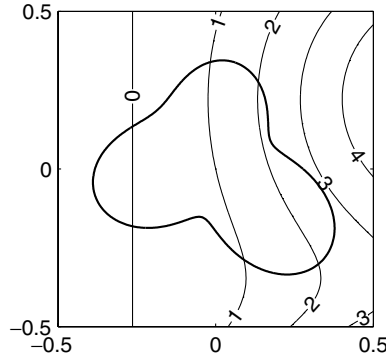


Fig. 2. Curve Γ with $(x_0, y_0) = (0, 0)$ plotted in computational domain $[-0.5, 0.5] \times [-0.5, 0.5]$. Contours of function $f(x, y)$ as defined in Eq. (24) plotted in the background.

where $\eta_{x,l}$ is such that $X_l = x_k + \eta_{x,l}h$, where $x_k \leq X_l < x_{k+1}$, and similarly for $\eta_{y,l}$. The relative error $E_{rel}^{cos} = |E^{cos}|/|\tilde{I}_{g,f}^T|$. The absolute value of the first moment is smaller than 0.025, and furthermore $\int_0^1 M_1(\varphi_2^{cos}, \eta) d\eta = 0$. The second moment is positive for all values of η , and $0.50 \leq M_2(\varphi_2^{cos}, \eta) < 0.55$.

In computing the different error terms, we find that in this case, the the $O(h)$ error term does not dominate over the first $O(h^2)$ error term for the values of h used here; the errors are rather similar in size. Sometimes these terms are of the same sign, sometimes the opposite. Therefore, we note the fluctuating convergence rates in Table 1. The errors in this table are computed as the average over 64 small irregular shifts in the grid. Individual realizations experiences large variations in measured convergence rates. See also the discussion regarding measured convergence rates in Section 2.

In Table 1, the curve Γ was discretized by $NC = 100$ points. As we increase the number of discrete points on the curve to $NC = 1000$, the scaled shifts relative to the closest grid point in $x(\eta_{x,l})$, and also in $y(\eta_{y,l})$ will have a more and more uniform distribution in $[0,1)$, and the fact that the first moment is of different sign at different points (since it integrates to zero), will make this error term smaller. Therefore, for the moderate values of the grid size h used here, the error term of second order will dominate, and we measure a convergence rate close to second order for δ_{2h}^{cos} , see Table 2.

For the hat functions and the piecewise cubic function, the first non-zero moment is monotone in sign as a function of η , and the first error term dominates over the second. The convergence of the errors in the tables, averaged over 64 small shifts in the grid, are very close to the predicted rates for both refinements. For individual realizations there are of course some variations, and also here we can note that as we increase NC from 100 to 1000 points, the variations decrease. For $NC = 100$, the measured convergence rates for the piecewise cubic function fluctuated between 3.48 and 4.71 for individual realizations, while for $NC = 1000$, measured convergence rates range from 3.94 to 4.06.

Table 2
As in Table 1, but with $NC = 1000$

δ_ε	Relative error (average)			Order of convergence	
	$N = 40$	$N = 80$	$N = 160$	P_{40-80}	P_{80-160}
δ_h^L	1.58×10^{-4}	4.03×10^{-5}	1.00×10^{-5}	1.97	2.00
δ_{2h}^L	6.42×10^{-4}	1.62×10^{-4}	4.04×10^{-5}	1.99	2.00
δ_{2h}^{cos}	4.25×10^{-4}	1.22×10^{-4}	3.12×10^{-5}	1.80	1.97
δ_{2h}^C	5.59×10^{-7}	3.43×10^{-8}	2.14×10^{-9}	4.03	4.00

In this section, we have demonstrated that for functions g and f with non-vanishing derivatives, we do numerically find the expected convergence rates for δ_h^L , δ_{2h}^L and δ_{2h}^C more closely as we average over a number of shifts in the grid. In the case of the cosine approximation δ_{2h}^{cos} we do not obtain as clean results, and we have discussed the reasons for this in detail.

Here, we have computed the integral over Γ with the trapezoidal rule, both for the computation of δ_ε (Eq. (22)) and for the line integral in Eq. (23). The choice of this quadrature rule for the integration over Γ is not essential, it can be replaced by any other quadrature rule. The total error compared to the analytical result $\int_\Gamma g(S)f(\mathbf{X}(S)) dS$ will be the error from the regularization as discussed above, plus the numerical error in evaluating this integral.

3.2. Regularization from distance function

A common technique for extending the regularized one dimensional delta function to several dimensions is to base the extension on the Euclidean distance to the singular set Γ . This is the standard procedure in connection to the level-set method since the distance function $d(\Gamma, x)$ is often readily available [9,13]. The multi-dimensional regularized delta function is then defined as

$$\delta_\varepsilon(\Gamma, \mathbf{x}) = \delta_\varepsilon(d(\Gamma, \mathbf{x})). \tag{25}$$

In [14,15], we showed that such a procedure, in connection to quadrature and the numerical solution of differential equations can be of high order accuracy if the support of the regularized delta function satisfies a number of moment and regularity conditions and if its support is allowed to grow relatively to the step size h as $h \rightarrow 0$, $\varepsilon \sim h^\alpha$, $0 < \alpha < 1$.

The choice of the support in practical level-set simulations has however mainly been $\varepsilon = h, 1.5h$ or $2h$, for discretization on regular grids [9,13]. We shall show that such a choice may result in $O(1)$ error.

Define a curve $\Gamma \in \mathbb{R}^2$, that is a straight line at an angle of 45° to the $x^{(1)}$ -axis; $\Gamma = \{x, x^{(1)} = x^{(2)}, 0 \leq x^{(1)} < \bar{S}/\sqrt{2}\}$. Consider the calculation of the length $|\Gamma|$

$$|\Gamma| = \bar{S} = \int_{\mathbb{R}^2} \delta(\Gamma, \mathbf{x}) d\mathbf{x} \tag{26}$$

computed using a δ_ε approximation on a regular grid,

$$\bar{S}_h = h^2 \sum_{\mathbf{j} \in Z^2} \delta_\varepsilon(d(\Gamma, \mathbf{x}_\mathbf{j})), \quad \mathbf{x}_\mathbf{j} = (x_{j_1}^{(1)}, x_{j_2}^{(2)}), x_{j_k}^{(k)} = j_k h, \quad j_k \in Z, \quad k = 1, 2. \tag{27}$$

If we divide the sum \bar{S}_h into contributions R_m related to M sub segments of Γ of length $\sqrt{2}h$ ($M = \bar{S}/(\sqrt{2}h)$), we have

$$\bar{S}_h = h^2 \sum_{m=1}^M R_m + h^2 \tilde{R}, \quad Mh = \bar{S}/\sqrt{2}.$$

The terms R_m , $m = 1, \dots, M$, corresponds to all values of $\delta_\varepsilon(d(\Gamma, \mathbf{x}_\mathbf{j}))$ with

$$\sqrt{2}(m-1)h \leq \mathbf{x}_\mathbf{j} \cdot (1/\sqrt{2}, 1/\sqrt{2}) < \sqrt{2}mh, \quad \mathbf{j} \in Z^2$$

and $\tilde{R} = O(h^{-1})$ contains the finitely many δ_ε -values from close to the end points of Γ .

For the piecewise linear hat function $\delta_\varepsilon = \delta_h^L$ using the fact that $\delta_\varepsilon(d(\Gamma, \mathbf{x}_\mathbf{j})) = 0$, for $d(\Gamma, \mathbf{x}_\mathbf{j}) \leq \varepsilon = h$, we have

$$R_m = \delta_h^L(0) + 2\delta_h^L(h/\sqrt{2}) = h^{-1} + 2h^{-1}(1 - 1/\sqrt{2}) = h^{-1}(3 - \sqrt{2}).$$

Summing all terms gives

$$\bar{S}_h = \frac{3 - \sqrt{2}}{\sqrt{2}} \bar{S} + O(h),$$

which results in a relative error $(|\bar{S}_h - \bar{S}|/\bar{S})$ of over 12% as $h \rightarrow 0$. Repeating the exercise for the wider piecewise linear hat function with $\varepsilon = 2h$ we have

$$\bar{S}_h = \frac{1}{4}(5\sqrt{2} - 3)\bar{S} + O(h),$$

which yields a relative error of 1.8% as $h \rightarrow 0$.

This $O(1)$ error occurs since the support of δ_ε , viewed along a grid line in x and y , will not be a multiple of grid points. In [15], we pointed out that a δ_ε discretization in one dimension with $2\varepsilon = \beta h$, β small but not an integer, leads to an $O(1)$ error. We also showed, that delta function approximations which yield the correct mass for any such dilation can be constructed. Such functions do not however have compact support. They have compact support in Fourier space, and decay exponentially in real space.

We now perform a numerical test to practically illustrate the results from above. Define the curve Γ as two parallel lines of length L at a normal distance $2a$, joined at both ends by a half circle of radius a . The angle of the lines to the x -axis is $\theta = \pi/4$. The total length of Γ is $\bar{S} = 2L + 2\pi a$. A sketch of Γ is plotted in Fig. 3, together with the distance function $d(\Gamma, \mathbf{x})$, for a specific choice of a and L .

We again define the relative error in the computation of the length of Γ as $E = |\bar{S}_h - \bar{S}|/\bar{S}$, with \bar{S} and \bar{S}_h as defined in Eqs. (26) and (27). In Table 3, the relative error E is displayed for different values of L and a , for different grid sizes h . Here, we have used the narrow piecewise linear hat function, δ_h^L . From the results in the table, we can see that we do not get any convergence as we decrease h . As a/L decreases, the error

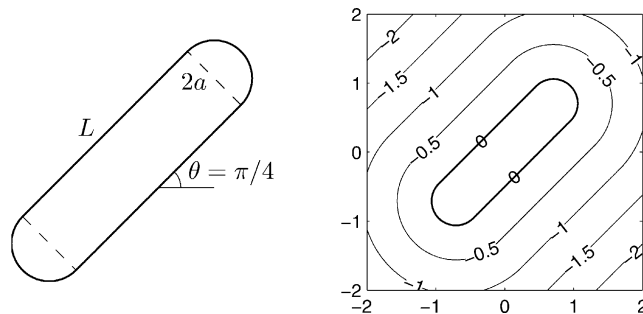


Fig. 3. Sketch of curve Γ . To the right the contours of the distance function to Γ defined with $L = 2$ and $a = \sqrt{2}/4$.

Table 3

The relative error $E = |\bar{S}_h - \bar{S}|/\bar{S}$, with \bar{S} and \bar{S}_h defined as in Eqs. (26) and (27) with Γ as shown in Fig. 3

L	a	Relative error		
		$h = 0.01$	$h = 0.005$	$h = 0.0025$
2.0	$0.24\sqrt{2}$	0.0803	0.0843	0.0793
2.0	$0.12\sqrt{2}$	0.0967	0.0966	0.0956
2.0	$0.06\sqrt{2}$	0.1079	0.1075	0.1068
2.0	$0.03\sqrt{2}$	0.1142	0.1140	0.1137
4.0	$0.03\sqrt{2}$	0.1174	0.1172	0.1176

The delta function approximation $\delta_\varepsilon = \delta_h^L$, the narrow hat function with $\varepsilon = h$.

Table 4

As in Table 3, but with the delta function approximation $\delta_\varepsilon = \delta_{2h}^L$, the wider hat function with $\varepsilon = 2h$

L	a	Relative error		
		h = 0.01	h = 0.005	h = 0.0025
2.0	0.24√2	0.0117	0.0119	0.0117
2.0	0.12√2	0.0142	0.0143	0.0140
2.0	0.06√2	0.0158	0.0158	0.0156
2.0	0.03√2	0.0167	0.0167	0.0166
4.0	0.03√2	0.0172	0.0172	0.0172

from the straight lines dominates more and more, and in the bottom of the table, we are approaching the relative error of 12% predicted for the straight lines.

In Table 4, we repeat the same computations for the wider hat function, δ_{2h}^L . The errors are smaller in this case, but also here, we have no convergence as h is decreased, and at the bottom of the table, we again approach the predicted relative error for the straight line, in this case 1.78%.

The O(1) errors that we are observing are not a result of the specific choice of the delta function approximation δ_ε , that is used to define $\delta_\varepsilon(d(\Gamma, \mathbf{x}))$, as was discussed above. For the piecewise cubic $\delta_{2h}^C \in Q^4$, numerical computations yield a relative error of 7.1% for all three h refinements for $L = 4.0, a = 0.03\sqrt{2}$. An O(1) error is to be expected for any δ_ε approximation with narrow compact support, since the problem is the dilation of its support in the grid line directions, as was discussed above.

This choice of Γ shows a special case with large errors. All local errors in the linear part of Γ have the same sign and no cancellation of errors occur. This case have been selected since it clearly illustrates the substantial O(1) errors that do exist.

In the case of a circle, cancellation of local errors will occur and the total error will be smaller, see Table 5. The errors fluctuate strongly depending on the location of Γ in the grid. Not even after averaging over many shifts of Γ with respect to the grid is there a regular behavior as a function of h . The table indicates a weak sub-linear convergence, for all three different choices of δ_ε .

3.3. Regularization of characteristic functions

Singularities of lower order than that of the delta function are common in computations of integrals and differential equations. Regularization of the characteristic function for a domain is used to represent piecewise constant or piecewise smooth functions [9,13,16,17].

We can develop discretely regularized characteristic functions based on the principles of Section 3.1 which produce high order of numerical accuracy. Let us define the characteristic function and its discretely regularized approximation

Table 5

The relative error E and order of convergence for different δ_ε functions used to define $\delta_\varepsilon(d(\Gamma, \mathbf{x}))$

δ_ε	Relative error (average)			Order of convergence	
	N = 40	N = 80	N = 160	P_{40-80}	P_{80-160}
δ_h^L	1.82×10^{-3}	1.27×10^{-3}	1.07×10^{-3}	0.51	0.26
δ_{2h}^L	3.31×10^{-4}	1.03×10^{-4}	1.76×10^{-4}	1.68	-0.77(< 0)
δ_{2h}^C	1.12×10^{-3}	8.67×10^{-4}	6.90×10^{-4}	0.43	0.33

The curve Γ is a circle of radius $0.35\sqrt{2}$.

The error has been computed averaging over 144 small irregular shifts of the circle Γ .

$$\chi(\Omega, \mathbf{x}) = \begin{cases} 1, & \mathbf{x} \in \Omega \subset \mathbb{R}^d, \\ 0, & \mathbf{x} \notin \Omega, \end{cases} \quad \chi_\varepsilon(\Omega, \mathbf{x}) = \int_{\Omega} \prod_{k=1}^d \delta_{\varepsilon k}(x^{(k)} - \xi^{(k)}) d\xi,$$

where $\delta_{\varepsilon k}$ is defined in Eq. (13) and we assume that Ω is bounded in \mathbb{R}^d and such that all integrals below are well defined. We can now derive an error estimate similar to that of Theorem 3 and we will use our notation from above.

Theorem 4. Suppose that $\delta_\varepsilon \in \mathcal{Q}^q, q > 0$, as in Definition 2.1, and $f \in C^r, r \geq q$. Then

$$E = \left| \int_{\mathbb{R}^d} \chi(\Omega, \mathbf{x}) f(\mathbf{x}) d\mathbf{x} - \left(\prod_{k=1}^d h_k \right) \sum_{\mathbf{j} \in Z^d} \chi_\varepsilon(\Omega, \mathbf{x}_j) f(\mathbf{x}_j) \right| \leq \mathbf{C} h^q$$

with $h = \max_{1 \leq k \leq d} h_k$ and $E = 0$ for constant f .

Proof. By definition, $\int_{\mathbb{R}^d} \chi(\Omega, \mathbf{x}) f(\mathbf{x}) d\mathbf{x} = \int_{\Omega} f(\mathbf{x}) d\mathbf{x}$. For the second term, we have that

$$\left(\prod_{k=1}^d h_k \right) \sum_{\mathbf{j} \in Z^d} \chi_\varepsilon(\Omega, \mathbf{x}_j) f(\mathbf{x}_j) = \int_{\Omega} \left[h_1 \sum_{j_1 \in Z} \delta_\varepsilon(x_{j_1}^{(1)} - \xi^{(1)}) \left[h_2 \sum_{j_2 \in Z} \dots \left[h_d \sum_{j_d \in Z} \delta_\varepsilon(x_{j_d}^{(d)} - \xi^{(d)}) f(\mathbf{x}_j) \right] \dots \right] \right] d\xi.$$

From here the proof follows analogously to that of Theorem 3, with the integral over Γ replaced by the integral over Ω . Note that the argument of δ_ε in this case is such that we obtain $f(\xi)$ instead of $f(\mathbf{X}(S))$ before.

The computation of χ_ε is more involved than that of the regularized delta function since the integration is over Ω . However, the support of δ_ε is narrow and thus integration is only needed in a band with a distance of order h to the boundary $\partial\Omega$ of Ω . In the domain interior of that band $\chi_\varepsilon \equiv 1$.

4. Differential equations with singular source terms

The properties of source term regularization in the numerical solution of differential equations are closely related to the regularization of singular integrands in numerical quadrature as discussed in Sections 2 and 3.

Let the solution of a differential equation

$$\begin{aligned} Lu &= s(\mathbf{x}), & \mathbf{x} \in \Omega \subset \mathbb{R}^d, \\ Bu &= r(\mathbf{x}), & \mathbf{x} \in \partial\Omega \end{aligned} \tag{28}$$

be given on the standard form as an integral of the fundamental solution $G(\mathbf{x}, \mathbf{y})$ multiplying the source term $s(\mathbf{x})$

$$u(\mathbf{x}) = \int_{\Omega} G(\mathbf{x}, \mathbf{y}) s(\mathbf{y}) d\mathbf{y} + R(\mathbf{x}), \tag{29}$$

where $R(\mathbf{x})$ represents the contribution from the boundary conditions. Let the solution of the corresponding numerical approximation have the form

$$u_j = \left(\prod_{k=1}^d h_k \right) \sum_{\mathbf{m} \in \Omega_h} G_{j\mathbf{m}} s_{\mathbf{m}} + R_j, \tag{30}$$

where $G_{j\mathbf{m}}$ is the discrete fundamental solution and Ω_h is the index set for the grid points inside Ω .

We will consider Eq. (29) with $s(\mathbf{y}) = \delta(\Gamma, g, \mathbf{y})$ for \mathbf{x} values away from the discontinuity and thus assume that $\delta(\Gamma, g, \mathbf{y})$ has compact support away from the boundaries and that $|\mathbf{x} - \mathbf{y}| \geq C > \varepsilon$ for any $\mathbf{y} \in \Gamma$. In the discrete approximation, we use a regularized delta function and define $s_{\mathbf{m}} = \delta_\varepsilon(\Gamma, g, \mathbf{x}_{\mathbf{m}})$ in Eq. (30). If we consider homogeneous boundary conditions, we have that $u(\mathbf{x})$ is given by Eq. (29) with $R(\mathbf{x}) = 0$ and u_j by Eq. (30) with $R_j = 0$ and where the summation over \mathbf{m} can be replaced by $\mathbf{m} \in Z^d$. We then have

$$\begin{aligned} |u(\mathbf{x}_j) - u_j| &= \left| \int_{\Omega} G(\mathbf{x}_j, \mathbf{y}) \delta(\Gamma, g, \mathbf{y}) \, d\mathbf{y} - \left(\prod_{k=1}^d h_k \right) \sum_{\mathbf{m} \in Z^d} G_{\mathbf{j}\mathbf{m}} \delta_\varepsilon(\Gamma, g, \mathbf{x}_{\mathbf{m}}) \right| \\ &\leq \left| \int_{\Omega} G(\mathbf{x}_j, \mathbf{y}) \delta(\Gamma, g, \mathbf{y}) \, d\mathbf{y} - \left(\prod_{k=1}^d h_k \right) \sum_{\mathbf{m} \in Z^d} G(\mathbf{x}_j, \mathbf{x}_{\mathbf{m}}) \delta_\varepsilon(\Gamma, g, \mathbf{x}_{\mathbf{m}}) \right| \\ &\quad + \left| \left(\prod_{k=1}^d h_k \right) \sum_{\mathbf{m} \in Z^d} [G(\mathbf{x}_j, \mathbf{x}_{\mathbf{m}}) - G_{\mathbf{j}\mathbf{m}}] \delta_\varepsilon(\Gamma, g, \mathbf{x}_{\mathbf{m}}) \right|. \end{aligned}$$

For the first part of the error, we can now identify the function f in Eq. (3) with the Greens functions above for fixed \mathbf{x}_j . The error analysis of Sections 2 and 3 will thus apply directly. If we assume $\delta_\varepsilon(\Gamma, g, \mathbf{x}_{\mathbf{m}})$ is defined as in Eq. (19), based on $\delta_\varepsilon(x), x \in \mathbb{R}$, where $\delta_\varepsilon(x) \in Q^q$, i.e., satisfies q moment conditions the error of the first part will be of $O(h^q)$.

Furthermore, if the numerical approximation is of order p with

$$|G_{\mathbf{j}\mathbf{m}} - G(\mathbf{x}_j, \mathbf{x}_{\mathbf{m}})| \leq C_1 h^p,$$

away from $\mathbf{x}_j = \mathbf{x}_{\mathbf{m}}$, then the total error

$$|u_j - u(\mathbf{x}_j)| \leq C_2 h^{\min(p,q)}, \tag{31}$$

where $|\mathbf{x}_j - \mathbf{x}| \geq C > \varepsilon$ for any $\mathbf{x} \in \Gamma$.

For $\delta_\varepsilon(\Gamma, \mathbf{x}) = \delta_\varepsilon(d(\Gamma, \mathbf{x}))$ (as in Eq. (25)), with $\varepsilon = mh$, no such estimate can be obtained. In fact, as shown in Section 3.2, there are cases where the quadrature error is $O(1)$. In Section 4.3, we perform a numerical test also for this approximation, solving the Poissons equation with a singular source term in 2D.

4.1. Ordinary differential equations

Now, consider a simple boundary value problem, including a delta function as the right hand side

$$\begin{aligned} -u_{xx} &= \delta(x - \bar{x}), \\ u(0) &= u(1) = 0, \end{aligned} \tag{32}$$

where $\bar{x} \in (0, 1)$. This equation has the solution

$$u(x) = G(x, \bar{x}) = \begin{cases} x(1 - \bar{x}), & 0 \leq x \leq \bar{x}, \\ \bar{x}(1 - x), & \bar{x} < x \leq 1, \end{cases}$$

where G is the Green's function. The solution can also be written

$$u(x) = \int_0^1 G(x, y) \delta(y - \bar{x}) \, dy.$$

Introducing a uniform grid with grid size $h = 1/N$ and grid points $x_j = jh$, $j = 0, \dots, N$, the equation is discretized by

$$-D_2 u_j = \delta_\varepsilon(x_j - \bar{x}), \quad j = 1, \dots, N-1, \quad u_0 = u_N = 0. \quad (33)$$

We discretize the second derivative using both a second and a fourth order approximation. For second order, set $D_2 = D_2^2$, where

$$D_2^2 u_j = (u_{j+1} - 2u_j + u_{j-1})/h^2 \quad (34)$$

and for the fourth order approximation, set $D_2 = D_2^4$, where

$$D_2^4 u_j = \begin{cases} (u_{j+4} - 6u_{j+3} + 14u_{j+2} - 4u_{j+1} - 15u_j + 10u_{j-1})/(12h^2), & j = 1, \\ (-u_{j+2} + 16u_{j+1} - 30u_j + 16u_{j-1} - u_{j-2})/(12h^2), & 2 \leq j \leq N-2, \\ (10u_{j+1} - 15u_j - 4u_{j-1} + 14u_{j-2} - 6u_{j-3} + u_{j-4})/(12h^2), & j = N-1. \end{cases} \quad (35)$$

For $\bar{x} = x_m$ and replacing $\delta_\varepsilon(x_j - x_m)$ in Eq. (33) by $h^{-1}\delta_{jm}$, where δ_{jm} is the Kronecker delta, the solution for the second order difference stencil is the discrete Greens function

$$G_{jm}^2 = \begin{cases} x_j(1 - x_m), & 0 \leq j \leq m, \\ x_m(1 - x_j), & m < j \leq N. \end{cases} \quad (36)$$

The solution for general \bar{x} is given by

$$u_j = h \sum_{m=0}^N G_{jm} \delta_\varepsilon(x_m - \bar{x}) \quad (37)$$

with $G_{jm} = G_{jm}^2$.

The function $G(x_j, x_m)$ is regular for $x_j \neq x_m$ and G_{jm}^2 is regular for $j \neq m$. By regular for the discrete function G_{jm}^2 is meant that it has bounded divided differences of arbitrary high order. The error $|u_j - u(x_j)|$ is given by an expansion of the form in Eq. (3) and the moment conditions for accuracy given in Proposition 1 apply. This discrete Greens function is piecewise linear, and for a δ_ε that obeys at least two moment conditions, i.e., $\delta_\varepsilon \in \mathcal{Q}^q$, $q \geq 2$, the numerical solution will therefore be exact (to round off error) away from the singularity. This is the case for example for the linear hat function. The cosine function $\delta_{2h}^{\cos} \in \mathcal{Q}^1$, and will have an $O(h)$ error. We will not discuss this low order approximation further.

In the upper row of Fig. 4, the error has been plotted for the second order discretization D_2^2 with δ_ε as δ_h^L , δ_{2h}^L and δ_{2h}^C . Away from the singularity, we have only round off errors. Close to the singularity, for δ_{2h}^L and δ_{2h}^C we have an $O(h)$ error at two grid points. This yields an $O(h)$ error if measured in maximum norm, and an $O(h^2)$ error if measured in 1-norm. For the narrow hat function, there is no peak in error at the singularity. The difference Eq. (33) with $D_2 = D_2^2$ and $\delta_\varepsilon = \delta_h^L$ yields $u_j = u(x_j)$, the exact solution to (32). This is a very specific property for this combination of difference stencil and δ_ε function. It can be seen by detailed truncation error analysis, see [2].

For the fourth order stencil D_2^4 in Eq. (35), the corresponding characteristic equation is

$$r^4 - 16r^3 + 30r^2 - 16r + 1 = (r-1)^2(r-7+\sqrt{48})(r-7-\sqrt{48}) = 0$$

with real roots $r_1 = r_2 = 1$, $r_3 = 7 - \sqrt{48} \approx 0.07$, $r_4 = 7 + \sqrt{48} \approx 13.93$, and the homogeneous solution is $u_j = a_1 + a_2 j + a_3 r_3^j + a_4 r_4^j$. The discrete Greens function is given by

$$G_{jm}^4 = \begin{cases} g_j^L = a_1^L + a_2^L j + a_3^L r_3^j + a_4^L r_4^j, & 0 \leq j \leq m, \\ g_j^R = a_1^R + a_2^R j + a_3^R r_3^j + a_4^R r_4^j, & m < j \leq N, \end{cases}$$

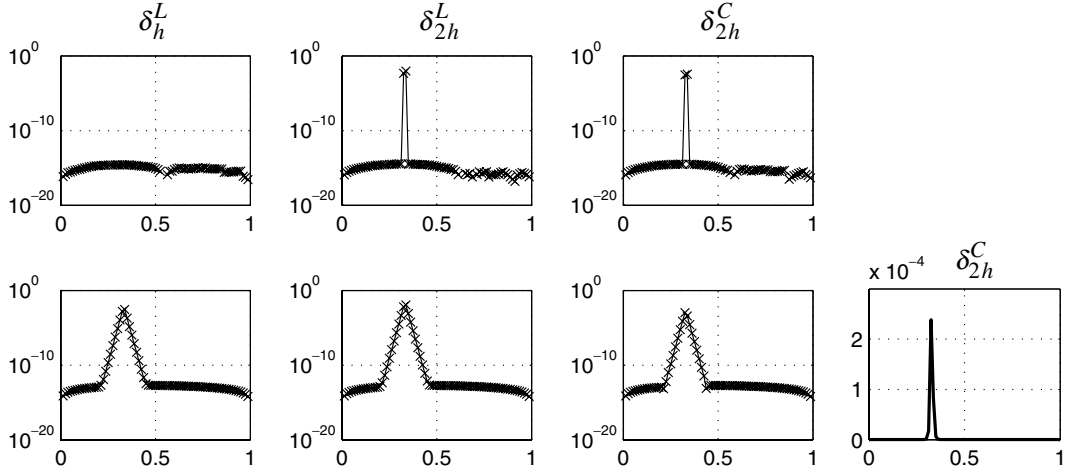


Fig. 4. Absolute value of the error of the numerical solution for $\bar{x} = 1/3$, computed with $N = 80$. Upper row: $D_2 = D_2^2$ (Eq. (34)); lower row: $D_2 = D_2^4$ (Eq. (35)). The columns are for different δ_ε functions; from left to right: δ_h^L , δ_{2h}^L and δ_{2h}^C . The extra plot on the right is again for δ_{2h}^C , D_2^4 , without the logarithmic scaling of the vertical axis.

To determine the coefficients, we need to solve $-D_4^2 G_{jm}^4 = \delta_{jm}$, where δ_{jm} is the Kronecker delta, with homogeneous boundary conditions. We have that $D_2^4 g_j^L = D_2^4 g_j^R = 0$, for $j = 2, \dots, N-2$, for any choice of the coefficients $a_1^L, \dots, a_4^L, a_1^R, \dots, a_4^R$. However, at $j = 1$ and $j = N-1$, the stencil is skew, and this is not the stencil for which the characteristic equation was derived. This puts conditions on the coefficients. It is also the case at $j = m-1$ and $j = m+1$, where the stencil will use a combination of values from the left and right solution. Furthermore, we have a continuity condition at $j = m$. In summary, the eight conditions that determine the coefficients are $D_2^4 G_{mm}^4 = -1/h$, $D_2^4 G_{jm}^4 = 0$ for $j = 1, m-1, m+1, N-1$, $G_{0m} = G_{Nm} = 0$ and $g_m^L = g_m^R$. Solving the full system yields long and complicated expressions for the coefficients. Ignoring exponentially small terms, an approximation to the discrete Greens function is given by

$$G_{jm}^4 = \begin{cases} x_j(1-x_m) - h(16r_4^3 - 31r_4^2 + 16r_4 - 1)^{-1} r_4^{j-m+3}, & 0 \leq j \leq m, \\ x_m(1-x_j) - h(16r_4^3 - 31r_4^2 + 16r_4 - 1)^{-1} r_4^{m-j+3}, & m < j \leq N, \end{cases}$$

where $r_4 = 7 + \sqrt{48}$, and we have used $r_3 = l/r_4$.

In difference to the second order approximation, for which the discrete Greens function as given in Eq. (36) is piecewise linear (the characteristic function in that case is $r^2 - 2r + 1 = (r-1)^2 = 0$ and the homogeneous solution is $u_j = a_1 + a_2 j$), it is in this case given by the same piecewise linear function plus a term that is exponentially small in most of the domain. The extra term has a maximum value proportional to h and it decays exponentially as a function of $|j-m|$.

The numerical solution is given by the sum in Eq. (37). The solution u_j at x_j is hence obtained by evaluating the value of G_{jm}^4 at (x_j, \bar{x}) by interpolation, where the δ_ε approximation determines the interpolation weights. The accuracy of the interpolation for x_j away from \bar{x} is controlled by the discrete moment conditions, and normally for $\delta_\varepsilon \in \mathcal{Q}^q$, this would yield an $O(h^q)$ error (Proposition 1). However, for this result to hold, the derivatives of the discrete Greens function must be bounded independently of h . This is however not the case, the p th derivative of G_{jm}^4 contains a term that is exponentially decaying, but that has a magnitude proportional to $h \cdot h^{-p}$. This yields an $O(h)$ exponentially decaying error independent of the moment order of the δ_ε function. Furthermore, the discrete Greens function G_{jm}^4 contains the exponentially decaying terms, and hence so does also the interpolated value at (x_j, \bar{x}) . Since the exact solution is equal to

the linear part of this Greens function, this also yields an $O(h)$ error that decays exponentially away from \bar{x} . In total, the $O(h)$ exponential terms will give essential contributions to the solution close to $x = \bar{x}$, see Fig. 4.

As was the case for the δ_h^L in combination with D_2^2 , also for the fourth order stencil, it is possible to derive a δ_ε function such that the difference Eq. (33) with $D_2 = D_2^4$ and this δ_ε function yields $u_j = u(x_j)$, the exact solution to Eq. (32). This function δ_{2h}^{LL} is given by Eq. (13) with $\varepsilon = 2h$ and the piecewise linear φ function

$$\varphi_2^{LL}(\xi) = \begin{cases} \frac{1}{12}(14 - 15|\xi|), & 0 \leq |\xi| \leq 1, \\ \frac{1}{12}(2 - |\xi|), & 1 < |\xi| \leq 2. \end{cases} \quad (38)$$

This function can be derived by a detailed truncation error analysis, taking care to expand the solution separately to the left and the right of \bar{x} . In the end, this leads to four conditions, involving four grid points $x_{m-1}, x_m, x_{m+1}, x_{m+2}$, where $\bar{x} = x_m + \eta h, 0 \leq \eta < 1$ that should hold for all η .

The δ_ε approximation δ_{2h}^{LL} obeys two moment conditions, i.e., $\delta_{2h}^{LL} \in \mathcal{Q}^2$. For equations where the Greens function is a general function with non-vanishing derivatives, this will limit the numerical order away from the singularity to second order, even if the finite difference approximation is of higher order, as given in Eq. (31). This will be shown numerically in Section 4.2.

Similar to the discussion in Section 2.2 for general quadrature formulas, there are examples where the support of the δ_ε function must be increased to accommodate certain difference stencils. Consider a simple model problem

$$\frac{du}{dx} = \delta(x - \bar{x}), \quad x > 0, \quad \bar{x} > 0, \quad u(0) = 0.$$

The fundamental solution and here also the solution is given by the Heaviside function $u(x) = H(x - \bar{x})$. The numerical method

$$Du_j = \delta_\varepsilon(x_j - \bar{x}), \quad j \geq 0, \bar{x} > \varepsilon, \quad u_0 = 0 \quad (39)$$

with $Du_j = D + u_j = (u_{j+i} - u_j)/(2h)$, has the solution $u_j = h \sum_{m=0}^{j-1} \delta_\varepsilon(x_m - \bar{x})$ and one moment condition is enough to guarantee full accuracy if $x_j < \bar{x} - \varepsilon$ or $x_j > \bar{x} + \varepsilon$. More generally, the solution u_j of (39) can be written using the discrete Greens function G_{jm}

$$u_j = h \sum_{m=0}^{\infty} G_{jm} \delta_\varepsilon(x_m - \bar{x}), \quad G_{jm} = \begin{cases} 0, & j \leq m, \\ 1, & j > m. \end{cases} \quad (40)$$

If we instead use centered differencing which has a wider stencil, i.e., let $D = D_0$ in Eq. (39), where $D_0 u_j = (u_{j+1} - u_{j-1})/(2h)$ the standard moment conditions do not imply accuracy. The discrete Greens function for this discretization solves Eq. (39) with $D = D_0$ and $\delta_\varepsilon(x_j - \bar{x})$ replaced by the Kronecker delta δ_{jm} , and it is not regular for $j > m$

$$G_{jm} = \begin{cases} 0, & j \leq m, \\ 2, & j > m, j - m \text{ odd}, \\ 1, & j > m, j - m \text{ even}, \end{cases} \quad (41)$$

since the divided difference $D + G_{jm}$ is not bounded as $h \rightarrow 0$. The discrete solution is given by the sum in Eq. (40), and with $\delta_\varepsilon = \delta_h^L$ the narrow hat function, we have an $O(1)$ error for $j > m$ if for example $\bar{x} = x_m$.

The fundamental solution G_{jm} in Eq. (41) can be seen as quadrature weights and the analysis of Section 2.2 apply. With the wider hat function $\delta_\varepsilon = \delta_{2h}^L$ we recover full accuracy away from the singularity.

4.2. Parabolic equations

Let us now consider the time dependent equation

$$u_t = u_{xx} + a\delta(x - \bar{x}(t)) \tag{42}$$

with $u(0, t) = u(1, t) = 0, u(x, 0) = 0$ and where $\bar{x}(t) \in (0, 1)$. Solutions to this equation with $a = 10$ are plotted in Fig. 5.

In space, we discretize u_{xx} either by the second order approximation D_2^2 (Eq. (34)), or the fourth order approximation D_2^4 (Eq. (35)). We use the explicit second order Runge–Kutta method (Heun’s method) in time, with a time step Δt . For stability reasons, we need $\Delta t \sim h^2$, and the time stepping error will therefore be $O(h^4)$. The δ_ε functions that we use are, as before, $\delta_h^L, \delta_{2h}^L$, and δ_{2h}^C . We also include δ_{2h}^{LL} as defined with φ_2^{LL} in Eq. (38).

Since we do not have an exact solution, we measure the numerical convergence using the difference of consecutively refined solutions. We compute with $(N, \Delta t) = (N_0, \Delta t_0), (2N_0, \Delta t_0/4)$, etc., with $N_0 = 20, \Delta t_0 = 2.5 \times 10^{-4}$, and N ranging from 20 to 320.

First, consider the case where the singularity location is constant in time, with $\bar{x} = 1/3$. From Fig. 6, we can note a first order convergence in maximum norm for the discretization choices δ_{2h}^L, D_2^2 and δ_{2h}^C, D_2^4 . For the discretization choices δ_h^L, D_2^2 and δ_{2h}^{LL}, D_2^4 , we observe a second order convergence in maximum norm. This is a very special property for these discretization pairs. As discussed in Section 4.1, these discretizations solve the boundary value problem in Eq. (32) to round off error. All these four discretizations have a second order convergence in 1-norm. For the cases where the maximum norm is $O(h)$ it is so over an interval of width $O(h)$, which yields an $O(h^2)$ term in the 1-norm. Now, introduce an interval

$$\tilde{I} = \{x : 0 \leq x < \bar{x} - \beta, \bar{x} + \beta < x \leq 1\}$$

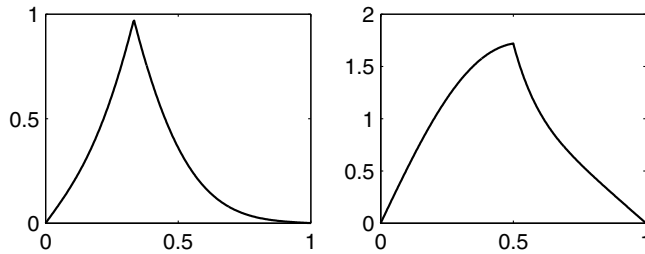


Fig. 5. Solutions to Eq. (42) with $a = 10$. Left frame: $t = 0.03, \bar{x} = 1/3$; right frame: $t = 0.2, \bar{x}(t) = 0.5 + 0.3 \sin(10\pi t)$.

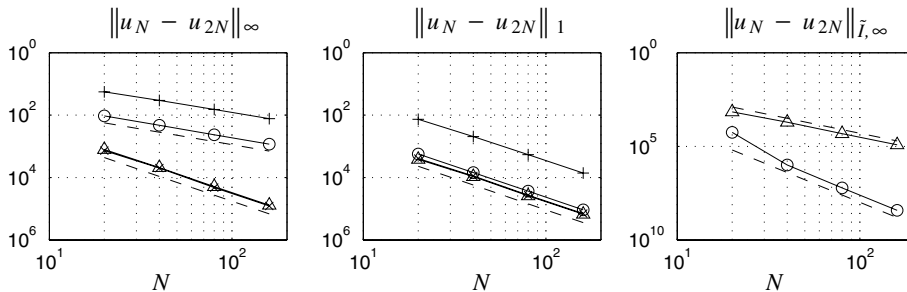


Fig. 6. Norms of difference of consecutive solutions plotted versus $N(\bar{x} = 1/3, t = 0.03)$. Discretizations: δ_h^L, D_2^2 (\times), δ_{2h}^L, D_2^2 ($+$), δ_{2h}^{LL}, D_2^4 (A), and δ_{2h}^C, D_2^4 (O). Dashed lines are proportional to; left plot: $1/N$ and $1/N^2$; middle plot: $1/N^2$; right plot: $1/N^2$ and $1/N^4$.

with $\beta = 0.1$, where we have cut away the region closest to \bar{x} . For the hat functions combined with the second order finite difference discretization, the maximum error measured over \tilde{I} is $O(h^2)$. This is the case also for δ_{2h}^{LL} combined with D_2^4 , as is shown in the right most plot in the figure. Even though D_2^4 is a fourth order approximation to the spatial derivative, this error is only second order since δ_{2h}^{LL} obeys only two moment conditions. Combining D_2^4 with the delta function δ_{2h}^C that obeys four moment conditions, this error is $O(h^4)$ as can be seen in the same plot.

Waldén [18] reported only second order convergence in a numerical simulation with a fourth order difference approximation of the heat equation coupled to a delta function regularization with four moment conditions satisfied. There was no explanation given and the result seems to contradict ours. We expect the reason for not achieving fourth order convergence rate away from the singularity comes from the initial values. In our example $u = 0$ initially but in [18] u had initial values with a discontinuity in the derivative. Waldén also notes that for large t -values there is fourth order convergence which would be consistent with the assumption that the second order error components originate from the initial values and then dissipate with time. For analysis of numerical errors in difference approximations of the heat equation with non smooth initial data, see [5].

Now, let $\bar{x}(t) = 0.5 + 0.3 \sin(10\pi t)$ in Eq. (42). Compared to the previous case with a constant \bar{x} , it is more difficult in this case to get clean numerical results for the convergence rates; the grid effects are more pronounced. With the choice above, we measure the error at $t = 0.2$, a time where $\bar{x}(t) = 0.5$ is at a grid point for all grid resolutions. The singularity has however passed over a large interval over time; from 0.5 to 0.8, then to 0.2, and back to 0.5 in a sinusoidal motion. For this time dependent singularity location, a second order maximum error is not achieved for any discretization pair. In all cases, there is now a first order error present. This component is however smaller for the discretization pairs D_2^2, δ_h^L and D_2^4, δ_{2h}^C , who had a second order maximum error in the case of a constant \bar{x} .

We find in general, that the larger errors close to the singularity spread somewhat more compared to the case of a fixed \bar{x} . In the right most plot in Fig. 7, we measure the error with $\beta = 0.2$ in the definition of \tilde{I} . Again, we find that the order of convergence for the discretization choice δ_{2h}^{LL}, D_2^4 is limited to second order, due to the moment order of δ_{2h}^{LL} even though the finite difference discretization is fourth order accurate. With δ_{2h}^C we have a fourth order convergence away from the singularity also in this case.

4.3. Elliptic equations

Let us consider the Poisson equation in \mathbb{R}^2

$$-\Delta u = \delta(\Gamma, \mathbf{x}), \quad \mathbf{x} \in \Omega \subset \mathbb{R}^2,$$

$$u(\mathbf{x}) = v(\mathbf{x}), \quad x \in \partial\Omega,$$

where $\Omega = \{x = (x, y); |x| \leq 1, |y| \leq 1\}$.

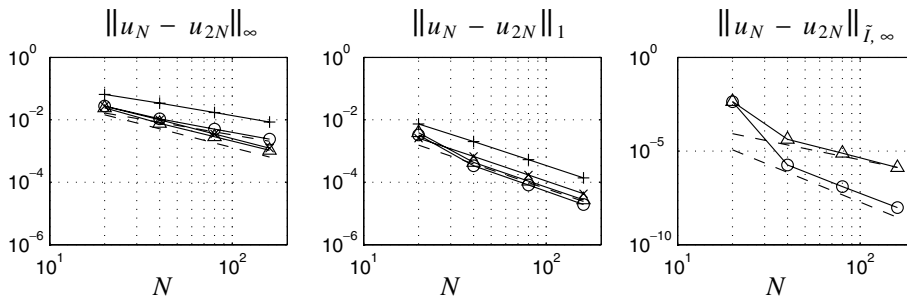


Fig. 7. As in Fig. 6, but with $\bar{x}(t) = 0.5 + 0.3 \sin(10\pi t)$ at $t = 0.2$. Dashed lines are proportional to; left plot: $1/N$ and $1/N^{3/2}$; middle plot: $1/N^2$; right plot: $1/N^2$ and $1/N^4$.

With Γ a circle, $\Gamma = \{\mathbf{x}, |\mathbf{x} - \bar{\mathbf{x}}| = 1/2\}$, and $v(\mathbf{x}) = 1 - \log(2|\mathbf{x} - \bar{\mathbf{x}}|)/2$, this equation has the following solution

$$u(\mathbf{x}) = \begin{cases} 1, & |\mathbf{x} - \bar{\mathbf{x}}| \leq 1/2, \\ 1 - \log(2|\mathbf{x} - \bar{\mathbf{x}}|)/2, & |\mathbf{x} - \bar{\mathbf{x}}| > 1/2. \end{cases} \quad (43)$$

This solution has been plotted in Fig. 8.

We introduce a uniform grid, with step size $h = 2/N$ in both x and y , i.e., with $(N + 1) \times (N + 1)$ grid points. As in Section 4.1, we use either second order stencil D_2^2 (Eq. (34)) or the fourth order stencil D_2^4 (Eq. (35)) to discretize the second derivatives.

The one dimensional delta function approximations are extended to two dimensions by the product rule in Eq. (22). We use $NC = 1000$ points to define the curve Γ . This fixed number of points is large enough for the resolution of the curve to be comparable to the grid resolution, also for the most refined grid that we will use.

To display how the error in the numerical solutions behaves close to Γ , we plot a cut of the error at $y = 0$ as a function of x in Fig. 9. The computations were done with $N = 160$, for $\bar{x} = 0$, for different combinations of the delta function approximation and finite difference approximations for the spatial derivatives. From left to right, we use δ_h^L combined with the second order finite difference approximation D_2^2 ; δ_{2h}^L again with D_2^2 ; and δ_{2h}^C together with the fourth order finite difference approximation D_2^4 .

The errors for the two hat functions δ_h^L and δ_{2h}^L are almost identical, except at a few points close to Γ , which for this cut is crossed at $x = -0.5$ and $x = 0.5$. Here, the properties of the narrow hat function when combined with D_2^2 as discussed above, reduces the error in these points, while the error for the wider hat function has a jump in one or two points close to Γ . For δ_{2h}^C with D_2^4 , the overall error is much lower, but it has a jump in the error close to Γ which is spread out over more points. This is due to the property of the wider finite difference stencil that was discussed in the previous section.

In the two left plots in Fig. 10, we show the error in maximum norm and $L1$ norm, as a function of N for these three discretization choices. The specific property of the combination δ_h^L and D_2^2 , as discussed in the previous section, does not hold perfectly in this case to yield an $O(h^2)$ maximum error, and also this maximum error is now $O(h)$. It does however reduce the maximum error, and it has almost as small maximum error as δ_{2h}^C combined with D_2^4 . An $O(h)$ error in a fixed number of points yields an $O(h^2)$ error when measured in $L1$ -norm.

For δ_{2h}^C , the error made in the points around Γ dominates the $L1$ -norm measure. To measure the error away from Γ , we introduce the sub-domain

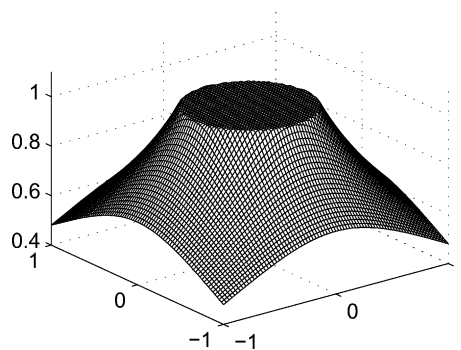


Fig. 8. Solution $u(\mathbf{x})$ as in Eq. (43) for $\bar{\mathbf{x}} = 0$.

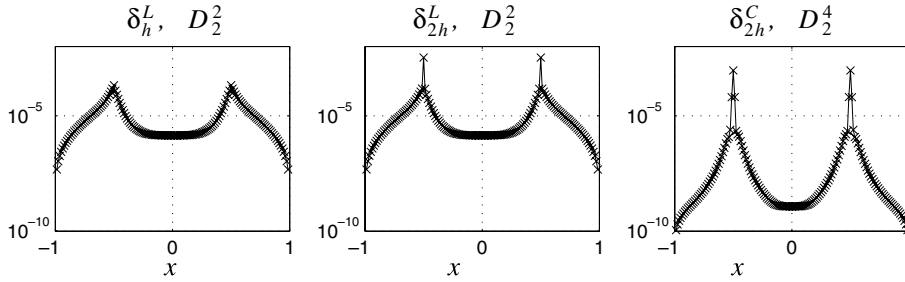


Fig. 9. Error for $y = 0$ plotted as a function of x , for different combinations of δ_ϵ and spatial discretizations. The δ_ϵ function have been extended to 2D using the product rule in Eq. (22). $N = 160$.

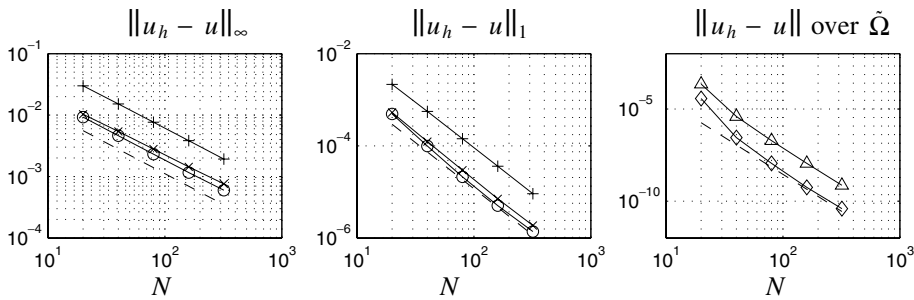


Fig. 10. In the two left figures, the max norm and 1-norm of the error are plotted for the three discretizations in Fig. 9: δ_h^L, D_2^2 (\times), δ_{2h}^L, D_2^2 ($+$), δ_{2h}^C, D_2^4 (\circ). In the right most frame, the maximum norm (Δ) and 1-norm (\diamond) as measured over $\tilde{\Omega}$ is plotted for δ_{2h}^C, D_2^4 . The dashed lines in the plots are from left to right proportional to $1/N$, and $1/N^2$ and $1/N^4$, respectively.

$$\tilde{\Omega} = \{\mathbf{x} : \mathbf{x} \in \Omega, |d(\Gamma, \mathbf{x})| > \beta\}.$$

We pick $\beta = 0.2$, which is $2h$ in the coarsest grid, and check the convergence in the maximum norm and $L1$ -norm when measured over this domain. The result is plotted in the right most frame in Fig. 10. We find a fourth order convergence as expected. For the first refinement, we get an artificially high convergence rate since β is not large enough for the coarsest grid to exclude the region where the exponentially decaying $O(h)$ error component is dominating. We need approximately $\beta = 4h$ to do so. For a shift in the grid, $\bar{\mathbf{x}} = (1/3 - 1/5, 1/3 - 1/5)$, such that $\bar{\mathbf{x}}$ is not a grid point at any resolution, the results are very similar.

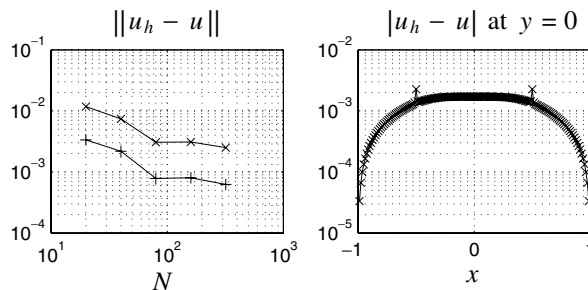


Fig. 11. In the left figure, the max norm (\times) and 1-norm ($+$) of the error are plotted for the discretization $\delta_{2h}^C(d(\Gamma, \mathbf{x})), D_2^4$. In the right figure, the error for $y = 0$ is plotted as a function of x , for $N = 160$.

In Section 3.2, we showed that narrow delta function approximations based on the distance to the curve, $\delta_\varepsilon(d(\Gamma, \mathbf{x}))$, does not yield accurate results when integrating over the delta function. This property is important also in the context of differential equations, as discussed above.

We now define $\delta_\varepsilon(\Gamma, \mathbf{x}) = \delta_{2h}^C(d(\Gamma, \mathbf{x}))$, and combine it with the fourth order spatial discretization. That is, we use the same one dimensional delta function, δ_{2h}^C , that was used above, but we extend the definition to two dimensions not by the product rule in Eq. (22), but instead by the closest distance to Γ . In this case, we can not establish even a first order convergence rate for the error in the maximum norm nor in the $L1$ -norm and, as is also shown in Fig. 11, the error away from Γ is much larger compared to when the product formula is used to define the delta function approximation.

5. Conclusions

In this paper, we have analyzed the accuracy of regularizations of Dirac delta functions, that can be used on standard computational grids in connection to numerical solution of differential equations with singular source terms and quadrature with singular integrands. The main contributions are in the analysis and development of techniques for multi-dimensional problems. We focus on the practically useful case of regularizations δ_ε with narrow support.

If the support is wide enough, so that δ_ε can be assumed to be well resolved on the grid, the error can be analyzed by splitting it into an analytical and a numerical part. This can be done also in several dimensions, where the δ_ε function is extended by using the distance function, s.t. $\delta_\varepsilon(\Gamma, \mathbf{x}) = \delta_\varepsilon(d(\Gamma, \mathbf{x}))$. The results regarding quadrature errors can be found in [14]. These results are related to the solution of partial differential equations, which has been further discussed in [15]. The optimal scaling will in general be algebraic, where the half width of the support $\varepsilon \sim h^\alpha$, $0 < \alpha < 1$.

In this paper, we have studied δ_ε functions with a more narrow support, where $\varepsilon = mh$ with m typically 1 or 2. Such approximations are the most common in practice. In this case, the δ_ε function is not resolved on the computational grid, and the discrete error must be analyzed directly. In one dimension, the discretization error of such a delta approximation is determined by the number of discrete moment conditions that this δ_ε function obeys (Proposition 1).

For partial differential equations in one spatial variable, the same discrete moment conditions, together with the order of the discretization, determine the accuracy away from the location of the singularity. Close to the singularity, an $O(h)$ error is to be expected, except in some special simple cases where some combinations of δ_ε function and difference stencils will yield an $O(h^2)$ error in the maximum norm.

We have discussed two different ways to extend the one dimensional δ_ε approximation to several dimensions; either by using the so called product rule in Eq. (19), or by the use of the distance function as in Eq. (25).

If the δ_ε function is extended to several dimensions by the distance formula, the result can have large errors. The possible failure has been illustrated by the computation of the length of a straight line at a 45° angle to the x -axis. With $\varepsilon = mh$, this error does not decrease with h . It is $O(1)$. To obtain convergence when extending the δ_ε function to several dimensions using approximations only based on the distance function, ε must be larger and chosen to scale algebraically with h [14,15]. Regularization based on the distance function is however very convenient for level-set methods. In order to avoid the $O(1)$ errors for narrow support regularization and still use the distance function we plan to let δ_ε also depend on the local angle between Γ and the coordinate axes. This will be the focus of a forthcoming paper.

For a δ_ε function extended to several dimensions by the product rule, we have proven that the quadrature error is bounded by Ch^q , where q is the number of discrete moment conditions that the one dimensional δ_ε function obeys (Theorem 3). The error for the solution to elliptic equations away from the singularity is, similarly to the error for PDEs in one space dimension, determined by these discrete moment

conditions, together with the order of the discretization. We have, for example, derived an approximation of the Poisson equation for which the error is $O(h)$ close to the singularity and $O(h^4)$ in the rest of the domain.

Acknowledgements

Research partially sponsored by Swedish TFR-Grant No. 222-2000-434.

References

- [1] J.T. Beale, A. Majda, Vortex methods II: higher order accuracy in two and three dimensions, *Math. Comput.* 39 (1982) 29–52.
- [2] R.P. Beyer, R.J. LeVeque, Analysis of a one-dimensional model for the immersed boundary method, *SIAM J. Num. Anal.* 29 (1992) 332–364.
- [3] A.J. Chorin, Numerical study of slightly viscous flow, *J. Fluid Mech.* 57 (1973) 785–796.
- [4] D. Juric, G. Tryggvason, A front-tracking method for dendritic solidification, *J. Comput. Phys.* 123 (1996) 127–148.
- [5] H.O. Kreiss, V. Thomée, O. Widlund, Smoothing of initial data and rates of convergence for parabolic difference equations, *Commun. Pur. Appl. Math.* 23 (1970) 241–259.
- [6] G. Ledfelt, A thin wire sub cell model for arbitrary oriented wires for the fd–td method, in: G. Kristensson (Ed.), *Proceedings of the EMB 98 – Electromagnetic Computations for Analysis and Design of Complex Systems*, 1998, pp. 148–155.
- [7] R.J. LeVeque, Z.L. Li, Immersed interface methods for stokes flow with elastic boundaries or surface tension, *SIAM J. Sci. Comput.* 18 (1997) 709–735.
- [8] J.J. Monaghan, Extrapolating B splines for interpolation, *J. Comput. Phys.* 60 (1985) 253–262.
- [9] S.J. Osher, R.P. Fedkiw, *Level Set Methods and Dynamic Implicit Surfaces*, Springer Verlag, Berlin, 2002.
- [10] C.S. Peskin, Numerical analysis of blood flow in the heart, *J. Comput. Phys.* 25 (1977) 220–252.
- [11] C.S. Peskin, The immersed boundary method, *Acta Numer.* 11 (2002) 479–517.
- [12] P.A. Raviart, An analysis of particle methods, in: *Lecture Notes In Mathematics*, Springer Verlag, Berlin, 1985, pp. 253–262.
- [13] J.A. Sethian, *Level Set Methods and Fast Marching Methods. Evolving Interfaces in Computational Geometry, Fluid Mechanics, Computer Vision and Materials Science*, Cambridge University Press, Cambridge, 1999.
- [14] A.K. Tornberg, Multi-dimensional quadrature of singular and discontinuous functions, *BIT* 42 (2002) 644–669.
- [15] A.K. Tornberg, B. Engquist, Regularization techniques for numerical approximation of PDEs with singularities, *J. Sci. Comput.* 19 (2003) 527–552.
- [16] A.K. Tornberg, B. Engquist, The segment projection method for interface tracking, *Commun. Pur. Appl. Math.* 56 (2003) 47–79.
- [17] G. Tryggvason, B. Bunner, A. Esmaeeli, D. Juric, N. Al-Rawahi, W. Tauber, J. Han, S. Nas, Y.J. Jan, A front-tracking method for the computations of multiphase flow, *J. Comput. Phys.* 169 (2001) 708–759.
- [18] J. Waldén, On the approximation of singular source terms in differential equations, *Numer. Meth. Part D E* 15 (1999) 503–520.